Sensors and Materials, Vol. 36, No. 11 (2024) 5049–5063
MYU Tokyo

S & M 3850

Configuration Optimization of Distributed Energy System Considering Multi-energy Complementary and Load Metering Devices: A Multi-objective Exponential Distribution Optimization Algorithm

Honghao Liu,[1] Tianyu Wen,[1] Cheng-Jian Lin,[2*] and Lingling Li[1]

[1]State Key Laboratory of Reliability and Intelligence of Electrical Equipment, Hebei University of Technology, Tianjin 300401, China
[2]Department of Computer Science & Information Engineering, National Chin-Yi University of Technology, Taichung 411, Taiwan

(Received July 19, 2024; accepted November 8, 2024)

Keywords: distributed energy system, multi-energy complementary, configuration optimization, multi-objective exponential distribution optimization algorithm, energy metering device

The combination of renewable energy technologies and distributed energy systems is an effective way to reduce carbon emissions and improve energy utilization. In this study, a multi-energy complementary distributed energy system (MC-DES) integrating photovoltaic, solar thermal collector, ground source heat pump, energy storage, and energy metering devices is proposed. The system employs sensor devices to measure the cooling, heating, and electric loads of the users and satisfies diversified energy demands through the synergistic operation of the energy supply and energy storage devices. To obtain the optimal capacity configuration scheme of MC-DES, a multi-objective configuration optimization model considering annual economic cost (AEC), primary energy consumption (PEC), and carbon dioxide emission (CDE) is established. A multi-objective exponential distribution optimizer (MOEDO) algorithm based on the fitness allocation mechanism and external archive maintenance mechanism is proposed to solve the configuration optimization problem. A hotel building is used as a case study to verify the effectiveness of the MOEDO algorithm, and the impact of different renewable energy technologies on the system performance is analyzed. The results show that compared with the conventional nondominated sorting genetic algorithm III (NSGA-III), multi-objective particle swarm optimization (MOPSO), and multi-objective evolutionary algorithm based on decomposition (MOEA/D) algorithms, the MOEDO algorithm reduces AEC of the MC-DES system by 3.42, 3.76, and 11.58%, while PEC is reduced by 3.44, 10.11, and 3.44% and CDE is reduced by 4.93, 11.20, and 1.58%, respectively. In addition, compared with the traditional separation production system, the economic, energy-saving, and environmental performances of the MC-DES are improved by 20.25, 58.62, and 68.44%, respectively.

*Corresponding author: e-mail: cjlin@ncut.edu.tw
https://doi.org/10.18494/SAM5249

ISSN 0914-4935
https://myukk.org/

1. Introduction

Energy is an important foundation for supporting social progress and development and is a matter of national livelihood. With the burgeoning economy and the ever-increasing population, the global energy consumption is increasing at a rapid pace, and the resulting environmental pollution problem is becoming increasingly severe.(1) The massive use of fossil energy has led to a severe greenhouse effect, with global carbon emissions reaching a record 35.8 billion tons in 2023.(2) Exploring renewable energy technologies and efficient energy supply systems has become an effective way to address global climate change and energy issues. As a supplement to the traditional centralized energy system, distributed energy systems (DESs) have emerged as a focal point for development in the energy field, offering advantages such as high flexibility, efficient energy utilization, and low carbon emissions, with the installed capacity of DES exceeding 10 GW in more than 30 countries.(3)

With the gradual maturity of new energy utilization technologies, renewable energy sources such as biomass, solar, geothermal, and wind energy have been widely introduced into DESs.(4) The DES can significantly reduce fuel consumption, energy supply costs, and carbon emissions through the coordination and complementarity of fossil fuel and renewable energy.(5) Rahdan *et al.*(6) investigated the application of distributed photovoltaic (PV) systems in different scenarios, and concluded that PV access can reduce the total cost by 1.4%. Kazemian *et al.*(7) designed two high-performance DESs, in which an organic Rankine cycle, absorption refrigeration system, and ground source heat pump (GSHP) were combined, and conducted economic analysis of both systems using response surface methodology. Lou *et al.*(8) constructed a DES coupling solar thermal collector (STC) and PV system, and examined the performance of the solar system using actual load and weather data of the Lhasa and Xi'an regions. The simulation results showed that the PV and STC technologies can reduce the carbon emission of the DES.

The installed capacity of the equipment directly affects the operational benefits of the DES; whether the DES can give full play to its multi-energy complementary advantages depends largely on the capacity configuration scheme. The configuration optimization methods for the DES are broadly categorized as either mathematical programming or intelligent optimization algorithms. Tian *et al.*(9) developed a mixed-integer planning model, which effectively enhances the flexibility of DES under various operational scenarios. Li *et al.*(10) optimized a distributed solar biogas energy system through mixed-integer linear programming (MILP) and Benders decomposition methods to determine the optimal design of the components within the system. However, when dealing with nonlinear, multidimensional, and multiconstraint DES optimization problems, the above mathematical planning methods suffer from the problem of long solution times.(11) Artificial intelligence algorithms with robust computing capabilities are becoming increasingly mainstream tools for optimizing DES configurations.(12)

Many researchers have used artificial intelligence algorithms to optimize DES. Kumar and Karthikeyan(13) applied the golden jackal optimization (GJO) algorithm to address the energy management problem of distributed microgrids and concluded that the GJO algorithm exhibits superior computational efficiency compared with traditional methods. Parvin *et al.*(14) optimized

three distributed systems in Iran using the multi-objective particle swarm optimization (MOPSO) algorithm with the objective of improving the power supply loss rate and energy cost, and proved that the access of wind and PV technologies can improve the economy. Yang *et al.*[15] constructed a capacity configuration model of DES considering the flexibility objective and applied the nondominated sorting genetic algorithm-II (NSGA-II) to solve it. The results showed that the optimized system can dynamically respond to diverse energy demands.

In summary, the combination of DES and renewable energy technologies, especially solar and geothermal energy technologies, is of great significance in enhancing the system operational performance and promoting the low-carbon energy transition. However, most of the studies have only considered the involvement of a single renewable energy source in energy supply, and fewer studies have been conducted on the DES that integrates multiple renewable energy technologies and energy storage. In addition, the performance of the current multi-objective optimization algorithms needs further improvement to cope with the difficult capacity allocation problems arising from the structural change of the DES.

In this study, a multi-energy complementary DES (MC-DES) coupling solar and geothermal energy is proposed, and a multi-objective exponential distribution optimizer (MOEDO) algorithm is designed to optimize the capacity configuration scheme of the MC-DES. The main contributions of this study are summarized as follows.

1. A novel MC-DES is proposed, in which PV, STC, GSHP, energy storage, and sensor devices are combined, and a multi-objective configuration optimization model considering energy, economic, and environmental benefits is constructed for MC-DES.
2. A novel MOEDO algorithm with the fitness allocation and external archive maintenance mechanism introduced into the exponential distribution optimizer (EDO) algorithm is proposed, and the practicality of the MOEDO algorithm is verified by comparing the results of different algorithms for solving the configuration optimization model.
3. The effects of different optimization algorithms and different renewable energy technologies on the performance of the DES are analyzed to verify the effectiveness of the proposed MC-DES.

The rest of this study is structured as follows. In Sect. 2, we describe the system architecture and establish the optimization model of the MC-DES. In Sect. 3, we propose the MOEDO algorithm. In Sect. 4, we conduct a case study to validate the effectiveness of the MC-DES and MOEDO algorithm. In Sect. 4, we summarize the conclusions and future perspectives.

2. System Model

2.1 System structure

In this section, we describe in detail the structural framework of MC-DES. Figure 1 shows the structure diagram of the MC-DES. As depicted in Fig. 1, the MC-DES proposed in this paper contains STC, PV system, GSHP, gas turbine (GT), heat exchanger (HE), heat storage tank (HST), heat recovery (HR), gas boiler (GB), absorption chiller (AC), battery, and energy metering devices.[16,17] Energy metering devices include the temperature sensor and electricity

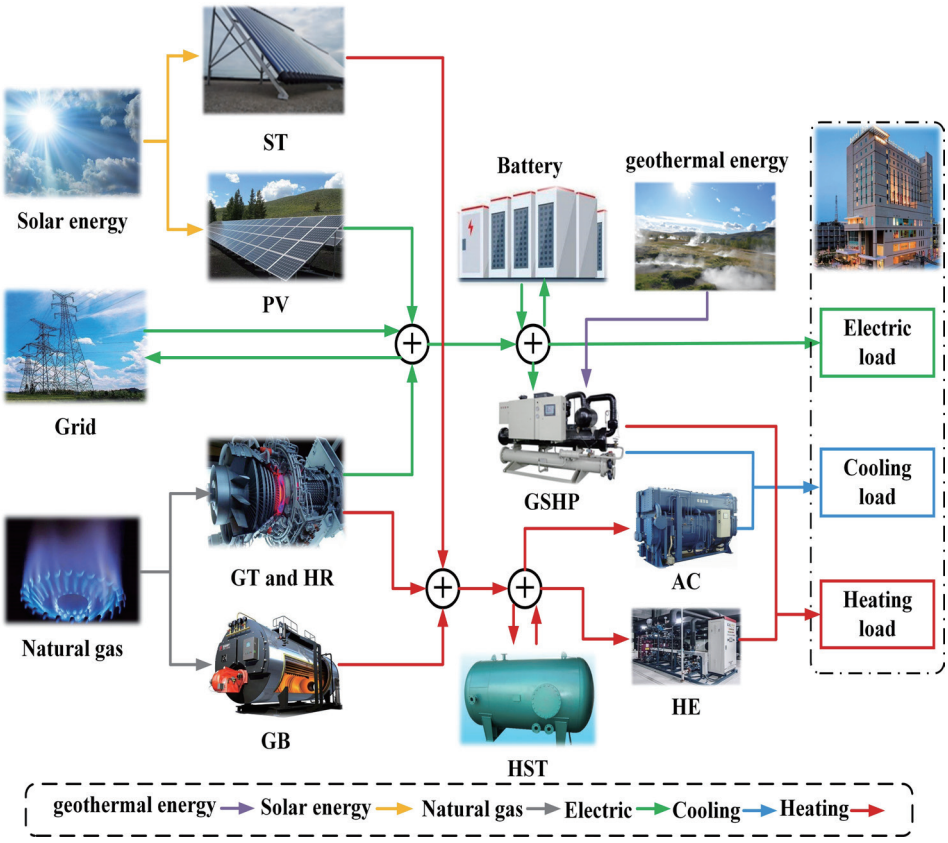

Fig. 1. (Color online) Structure diagram of the MC-DES.

sensor. The temperature sensor is used to measure the cooling and heating loads, while the electricity energy sensor is used to measure the electric load of the users. The coupling and complementation of natural gas, geothermal energy, and solar energy can be realized by reasonably coordinating the operation of different equipment. The PV system and STC convert solar energy into electrical and thermal energy required by users, respectively. GSHP utilizes geothermal energy for efficient cooling or heating. GT is driven by natural gas, which is used in conjunction with HR, AC, and HE to realize energy cascade utilization. HST and batteries are used as energy storage units to improve the matching of energy on the supply side and the demand side through rational charging and discharging of energy. GB is used to burn natural gas for supplemental heating when other equipment is unable to meet the heating load demand.

The stable energy supply characteristic of GSHP makes up for the insufficient output of STC, while PV provides the necessary electric power to drive GSHP, realizing complementarity between geothermal energy and solar energy. Natural gas drives equipment such as GT and GB and supplements the energy needs that cannot be met by renewable energy technologies to ensure the energy supply reliability of the MC-DES. This deep integration of traditional energy and renewable energy sources reduces dependence on fossil fuels, thereby effectively reducing carbon emissions while improving economic benefits.

2.2 Multi-objective optimization model

2.2.1 Decision variables

The decision variables for the MC-DES optimization problem include the installed capacities of GT, GB, AC, and batteries, the installed area of PV and ST, and the heating output ratio and cooling output ratio of GSHP. The decision variables can be integrated as

$$X_{de} = \left[IC_{GT}, IC_{GB}, IC_{HST}, IC_{Bat}, IA_{PV}, IA_{STC}, k_{gshp,c}, k_{gshp,h} \right], \tag{1}$$

where IC_{GT}, IC_{GB}, IC_{HST}, and IC_{Bat} are the installed capacities of GT, GB, HST, and batteries; IA_{STC} and IA_{PV} are the installed areas of STC and PV; and $k_{gshp,c}$ and $k_{gshp,h}$ are the cooling output ratio and heating output ratio of GSHP, respectively.

2.2.2 Objective functions

The primary energy consumption (PEC), annual economic cost (AEC), and carbon dioxide emission (CDE) of the MC-DES are set as the objective functions from the three perspectives of economy, environment, and energy.

PEC of the MC-DES can be expressed as

$$PEC = \sum_{t=1}^{T} (F_{GT,t} + F_{GB,t} + F_{grid,t}), \tag{2}$$

where $F_{GB,t}$, $F_{GT,t}$, and $F_{grid,t}$ are the fuel consumptions of the *GB*, *GT*, and grid at time *t*, respectively.

AEC of the MC-DES is

$$AEC = \sum_{t=1}^{T} (F_{s,t} \cdot C_g + E_{Buy,t} \cdot C_{e,Buy} - E_{Sell,t} \cdot C_{e,Sell}) + \sum_{l=1}^{n} C_l \cdot N_l \cdot \frac{d(1+d)^m}{(1+d)^m - 1}, \tag{3}$$

where C_g and $F_{s,t}$ represent the unit price per cubic meter of natural gas and the total amount of natural gas consumed, respectively. $E_{Buy,t}$ and $E_{Sell,t}$ denote the electricity purchased and sold at time *t*, respectively, and the corresponding prices per kWh are represented by $C_{e,Buy}$ and $C_{e,Sell}$. N_l and C_l represent the unit cost and installation capacity of the *l*-th equipment, respectively. *d* and *m* represent the discount rate and the service life of the device, respectively, where *d* is set as 0.06 and *m* is set as 20.

CDE of the MC-DES is

$$CDE = \sum_{t=1}^{T} \left[E_{Buy,t} \cdot \gamma_{\mathrm{CO2},e} + \left(F_{GT,t} + F_{GB,t} \right) \cdot \gamma_{\mathrm{CO2},g} \right], \tag{4}$$

where $\gamma_{\mathrm{CO2},e}$ and $\gamma_{\mathrm{CO2},g}$ are equivalent CO_2 emission factors for electricity and gas, respectively.

2.2.3 Constraint condition

The MC-DES needs to satisfy energy balance constraints during operation to maintain the balances of supply and demand for electricity, cooling, and heating. The energy balance constraints are shown as

$$E_{PV,t} + E_{B,dis,t} + E_{GT,t} + E_{Buy,t} = E_{gshp,t} + E_{B,ch,t} + E_{load,t} + E_{Sell,t}, \tag{5}$$

$$Q_{STC,t} + Q_{HST,dis,t} + Q_{GB,t} + Q_{GT,t} = Q_{AC,t} + Q_{HST,ch,t} + Q_{HE,in,t}, \tag{6}$$

$$C_{gshp,t} + C_{AC,t} = C_{load,t}, \tag{7}$$

where $E_{PV,t}$ and $E_{GT,t}$ are the electrical power outputs from PV and GT, respectively. $E_{B,dis,t}$ and $E_{B,ch,t}$ are the discharging and charging powers of the battery, respectively. $E_{Buy,t}$ and $E_{Sell,t}$ are the amounts of electricity purchased and sold by MC-DES, respectively. $E_{load,t}$ and $E_{gshp,t}$ are the electrical power consumed by the user and GSHP, respectively. $Q_{HST,dis,t}$ and $Q_{HST,ch,t}$ are the heat release and heat storage power of the HST, respectively. $Q_{STC,t}$ and $Q_{GB,t}$ are the thermal power generated by STC and GB, respectively. $Q_{GT,t}$ is the thermal power output from the GT. $Q_{HST,ch,t}$ and $Q_{HE,in,t}$ are the thermal power inputs to AC and HE, respectively. $C_{gshp,t}$ and $C_{AC,t}$ are the cooling power supplied by GSHP and AC, respectively; and $C_{load,t}$ is the cooling power consumed by the user.

3. Optimization Method

The configuration optimization of the MC-DES is a typical high-dimensional multi-objective optimization problem involving complex constraints and multiple decision variables and requires multi-objective algorithms with strong optimization-searching ability to solve. EDO algorithm is a new intelligence algorithm proposed in 2023, which performs optimization by simulating the mathematical formulas and basic properties of the exponential distribution model.[18] However, the EDO algorithm cannot handle multi-objective optimization problems effectively. Therefore, we propose MOEDO algorithm that is an improved version of the EDO algorithm. In this section, the algorithm improvement strategies are described in detail.

3.1 Fitness allocation mechanism

Multi-objective optimization problems cannot judge the superiority of solutions by comparing the magnitude of a single objective value. Therefore, a fitness allocation mechanism is introduced into the EDO algorithm to judge the advantages and disadvantages of different solutions by comparing the fitness values. The fitness value of an individual consists of two components, raw fitness and density information, which are calculated as follows:

$$Fit(i) = Ra(i) + De(i), \tag{8}$$

$$Ra(i) = \sum_{i \in P_m + \overline{P}_m \wedge j \prec i} S(i), \tag{9}$$

$$S(i) = \left| \left\{ j \mid j \in P_m + \overline{P}_m \wedge j \prec i \right\} \right|, \tag{10}$$

$$De(i) = \frac{1}{\delta_i^k + 2}, \tag{11}$$

$$k = \sqrt{N + N_a}, \tag{12}$$

where $Fit(i)$ denotes the fitness value of individual i in the population; $Ra(i)$ is the original fitness of an individual, which is determined by the dominance relationship between individuals; and $De(i)$ is the density information of an individual, which is determined by the distance between individuals. P_m and $\overline{P}_m$ denote the population and external archive of the MOEDO algorithm, respectively. δ_i^k is the distance between individual i and the k-th nearest individual to it; and N and N_a are the sizes of the population and external archive, respectively.

3.2 External archive maintenance mechanism

The algorithm needs to retain the nondominated solutions through an external archive with a specific size, but the situation that the number of nondominated solutions exceeds the size of the external archive may occur in the algorithm iteration. Therefore, we introduce an external archive maintenance mechanism in the EDO algorithm for maintaining the size of the archive. When the external archive is updated, individuals with fitness values less than 1 are preferentially copied to the next-generation archive.

$$\overline{P}_m^{t+1} = \{ i \mid i \in P_m + \overline{P}_m \wedge Fit(i) < 1 \} \tag{13}$$

If the number of individuals in the archive $\overline{P}_m$ is less than the archive size ($\left|\overline{P}_m^{t+1}\right| < N_a$), $N_a - \left|\overline{P}_m^{t+1}\right|$, excellent individuals with lower fitness are selected from the previous generation of the population and the external archive and copied to $\overline{P}_m^{t+1}$. If the number of individuals in $\overline{P}_m^{t+1}$ is greater than the archive size ($\left|\overline{P}_m^{t+1}\right| > N_a$), some individuals in $\overline{P}_m$ are deleted to maintain the archive size. The individual with the smallest distance from other individuals is preferentially deleted.

4. Case Analysis

4.1 Basic data

In this study, a hotel building located in Hebei, China, is selected as a case study, and the load demand of the building is satisfied by the MC-DES. The annual load of the hotel building is shown in Fig. 2. The electricity prices during peak (18:00–21:00), flat (10:00–15:00), and valley (23:00–07:00) periods are 0.18, 0.11, and 0.05 $/kWh, respectively.[19,20] The MOEDO algorithm is applied to optimize the configuration scheme of the MC-DES. To verify the practicality and effectiveness of the proposed MOEDO algorithm in the optimal configuration problem of the MC-DES, three classical algorithms, nondominated sorting genetic algorithm III (NSGA-III), multi-objective evolutionary algorithm based on decomposition (MOEA/D), and MOPSO, are selected for comparison. The maximum capacity for both the external archive and population in the algorithms is set to 100, and the maximum number of iterations is set to 200.

4.2 Analysis of optimization results of different algorithms

Figure 3 illustrates the Pareto fronts obtained by solving the optimized model of the MC-DES with different algorithms. From Fig. 3, it is evident that all algorithms successfully generate a range of feasible solutions for addressing the configuration optimization problem of the MC-DES, but there are differences in the distribution of the resulting Pareto front. The MOEA/D

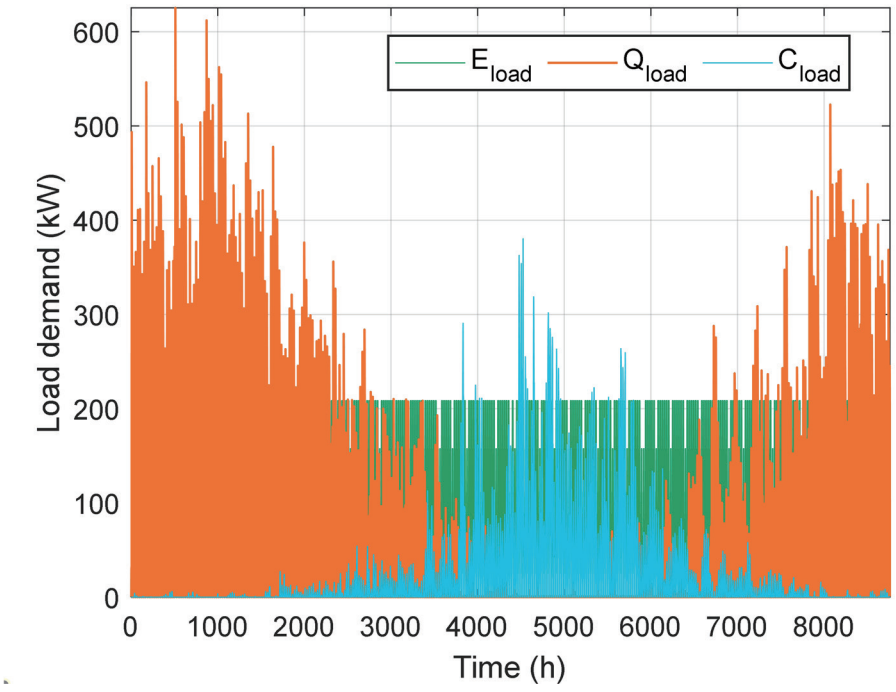

Fig. 2. (Color online) Annual load curve diagram.

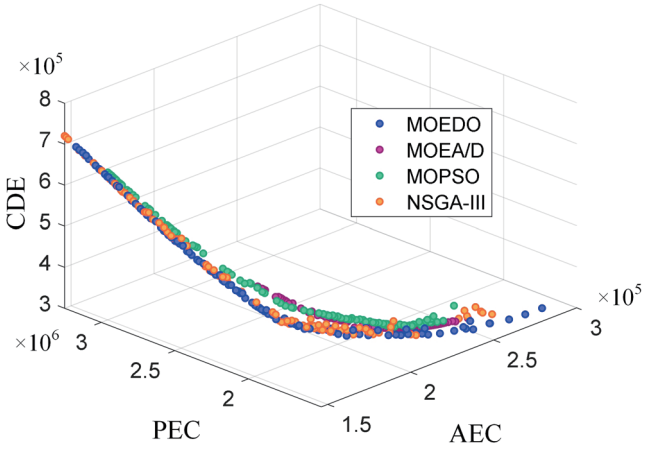

Fig. 3. (Color online) Pareto frontiers obtained by different algorithms.

algorithm exhibits the smallest coverage of the Pareto solutions, concentrating only on a limited part of the solution space, indicating that the diversity of the configuration schemes obtained by the MOEA/D algorithm is insufficient. The MOPSO and NSGA-III algorithms are roughly comparable to MOEDO in terms of solution set coverage, but inferior to MOEDO in terms of solution set quality and continuity, respectively. The solutions obtained by MOPSO are farther away from the axes, indicating that the resulting configurations have higher AEC, CDE, and PEC. The continuity of the frontiers obtained by the NSGA-III algorithm is poor, indicating that the algorithms have an insufficient search capability, which may lead to the omission of optimal solutions. Therefore, the proposed MOEDO algorithm significantly outperforms the other three algorithms in terms of the distribution range and continuity of the Pareto front, proving that the MOEDO algorithm can provide more diversified and high-quality configuration schemes for the MC-DES.

The technique for order preference by similarity to an ideal solution (TOPSIS) method is employed to select the optimal configuration scheme from the Pareto solution set obtained by the various algorithms. The optimal configuration schemes obtained by the MOEDO, MOPSO, NSGA-III, and MOEA/D algorithms are indicated in Table 1. The corresponding AEC, PEC, and CDE for each system configuration scheme are indicated in Table 2. A comparison of the configuration schemes in Table 1 reveals significant differences in the results produced by the various algorithms. The MOEDO algorithm recommends more PV, while the other algorithms advocate the installation of larger STC. In terms of energy storage devices, the MOEDO algorithm calls for a much larger capacity of HST than the other algorithms, while MOEA/D indicates the largest capacity of storage batteries.

Table 2 shows the AEC, PEC, and CDE of the MC-DES optimized with different algorithms. In terms of economy, the MC-DES optimized by the MOEDO algorithm reduces the AEC by 11.58, 3.76, and 3.42% compared with the MC-DES optimized by MOEA/D, MOPSO, and NSGA-III algorithms, respectively. In terms of energy efficiency, the configuration scheme obtained using the MOEDO algorithm has the least fuel consumption with a PEC of 2447493.97 kWh, which is reduced by 1.39, 10.11, and 3.44% compared with the schemes provided by the

Table 1
Configuration schemes obtained by different algorithms.

Items	MOEDO	MOEA/D	MOPSO	NSGA-III
GT capacity /kW	199	190	161	156
PV capacity /m^2	400	390	320	392
STC capacity /m^2	389	488	433	437
Battery capacity /kW	110	187	62	0
HST capacity /kW	690	307	447	521
GB capacity /kW	549	505	486	518
Heating ratio of GSHP	0.37	0.41	0.35	0.41
Cooling ratio of GSHP	0.30	0.63	0.38	0.21

Table 2
Optimization results of different algorithms.

Algorithm	AEC /$	PEC /kWh	CDE /kg
MOEDO	167104.07	1737817.41	384768.09
MOEA/D	188996.23	1762356.67	390946.64
MOPSO	173639.60	1933084.17	433309.17
NSGA-III	173023.77	1799771.76	404724.16

MOEA/D, MOPSO, and NSGA-III algorithms, respectively. In terms of environmental performance, the annual CDE of the MC-DES optimized by the MOEDO algorithm is 384768.09 kg, which is lower than that of the MC-DES optimized by the other algorithms. In summary, the MOEDO algorithm proposed in this paper can not only provide diversified configuration schemes for the MC-DES, but also, the resulting configuration schemes have strong competitiveness in terms of energy efficiency, economy, and environmental sustainability.

To verify the energy supply reliability of the MC-DES under the optimized configuration scheme obtained, two typical days are selected to analyze the energy balances and operation status of the MC-DES over a 24-hour period. The energy balances of the MC-DES system in winter and summer are shown in Figs. 4 and 5, respectively.

Figure 4 shows the energy balance state of the MC-DES on a typical winter day. As depicted in Fig. 4(a), the operating state of the GT depends on the electricity demand of users as well as the power generation of the PVs. During the periods of 01:00–07:00 and 22:00–24:00, the electricity demand of users is low and the PV output is zero, and all the electricity demand is satisfied by the GT. The PV generates electricity continuously during the period of 08:00–17:00 and takes up all the power supply tasks of the MC-DES during 10:00–16:00. In addition, since the power generated by the PV during 10:00–16:00 exceeded the electricity demand, part of the excess power was consumed by the battery while the remainder was sold to the grid. Figure 4(b) shows the heat energy balance of the MC-DES in winter. The heating demand to be matched by the system in winter consists of two parts, the majority of which is the heat demand of the users, and a small part of which is the heat consumed by AC cooling. Because of the low temperature and solar radiation intensity in winter, STC produces relatively little heat, and the MC-DES relies mainly on GT, GSHP, and GB for heat supply. During 01:00–09:00 and 17:00–24:00, the heat production of GT and GSHP meets most of the heating demand. During 10:00–16:00, GT stops working, and the MC-DES is mainly supplied with heat through HST and GB.

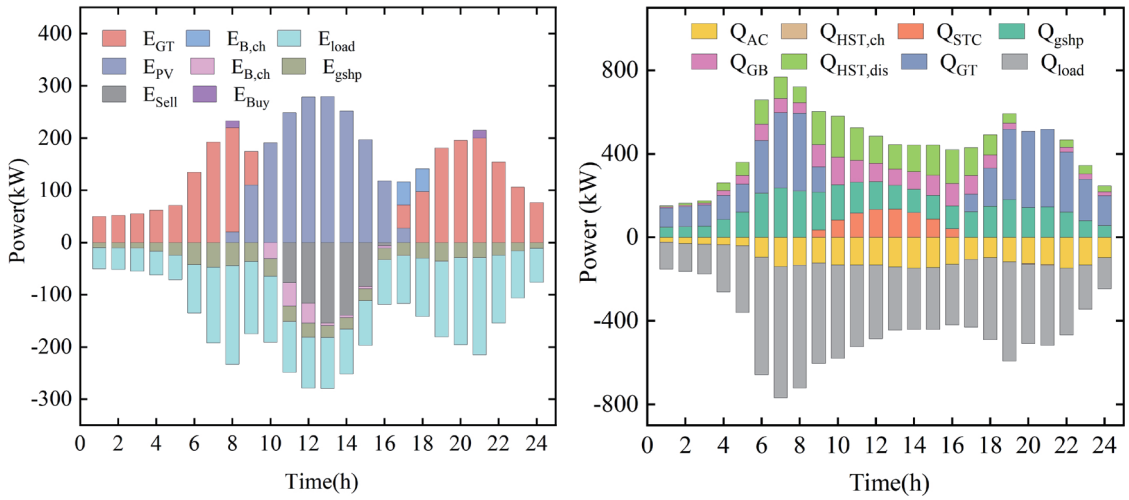

(a) (b)

Fig. 4. (Color online) (a) Electric and (b) heating energy balances of MC-DES on a typical winter day.

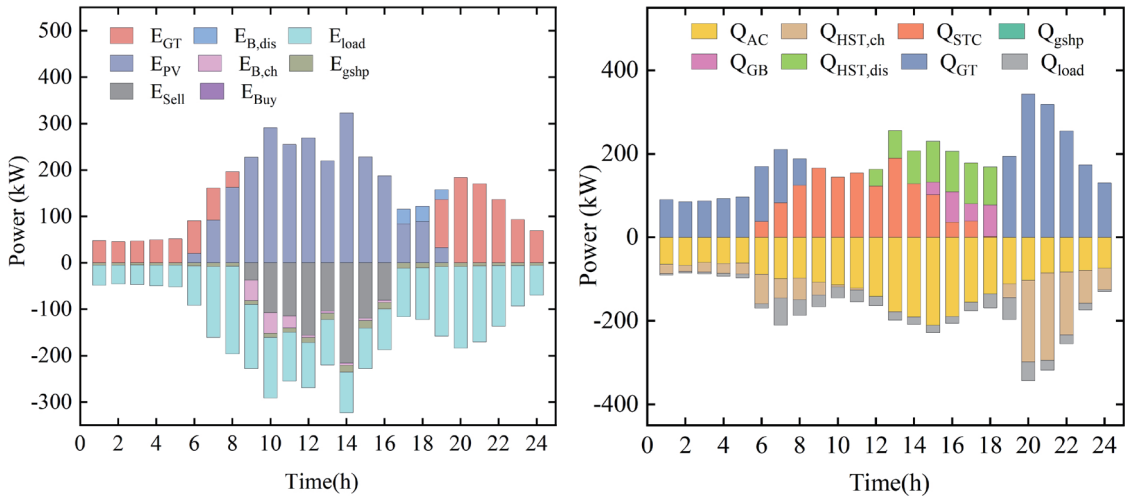

(a) (b)

Fig. 5. (Color online) (a) Electric and (b) heating energy balances of MC-DES on a typical summer day.

Figure 5 illustrates the energy balances of the MC-DES on a typical summer day. As illustrated in Fig. 5(a), the output power and operational hours of PV are significantly greater in summer than in winter, which decreases the output power of GT. Thanks to the increased power generation of PV, the MC-DES does not require electricity purchases from the grid on a typical summer day. Figure 5(b) presents the operation status of the heating device on a summer day. The heating demand in summer is much lower than that in winter, and the thermal energy required for AC cooling accounts for 83.3% of the total heating demand. During the summer months, the GSHP operates in the cooling mode and is unable to provide heat to the users, so the MC-DES relies heavily on the STC and GT for heat supply. Owing to the increased daylight hours in the summer, the STC operating hours are extended from 09:00–16:00 to 06:00–17:00,

enabling more heat to be produced. Since the peaks of heat demand and electricity demand on a typical summer day occur at different times, the GT produces heat in excess of user demand during some hours. To effectively utilize this excess heat, the HST always maintains heat storage from 01:00–9:00 and 19:00–24:00. In summary, the MC-DES effectively balances energy supply and demand, avoiding both energy shortages and wasteful conditions. This demonstrates the rationality of the configuration scheme obtained through the MOEDO algorithm.

4.3 Comparison of different DES models

To analyze the impact of the introduction of geothermal and solar energy equipment on the DES, four different systems are selected for optimal configuration, and their economic, energy-saving, and environmental performances are evaluated. Four cases are set up for comparative experiments, and all cases are optimized by the MOEDO algorithm.

Case 1: DES with PV, ST, and GSHP (i.e., MC-DES proposed in this study).
Case 2: DES with ST and GSHP, without PV.
Case 3: DES with PV and GSHP, without ST.
Case 4: DES with PV and ST, without GSHP.

To evaluate the performance of different systems more accurately, the traditional separate production (SP) system is deployed as the reference, and the economic cost saving rate (ECSR), CDE reduction rate (CDERR), energy saving rate (ESR), and performance comprehensive index (PCI) are selected as the performance evaluation indexes. The configuration scheme and system performance under different scenarios are shown in Fig. 6.

Figure 6(a) demonstrates the optimal equipment configuration scheme after the optimization of different systems. The configured capacities of GB and STC for Case 4 are significantly higher than in the other cases owing to the lack of GSHP with high heat production efficiency. The DES of Case 2 is not configured with PV, so the system has no excess power output and the installed capacity of the battery is 0. The configuration schemes of Case 3 and Case 1 have

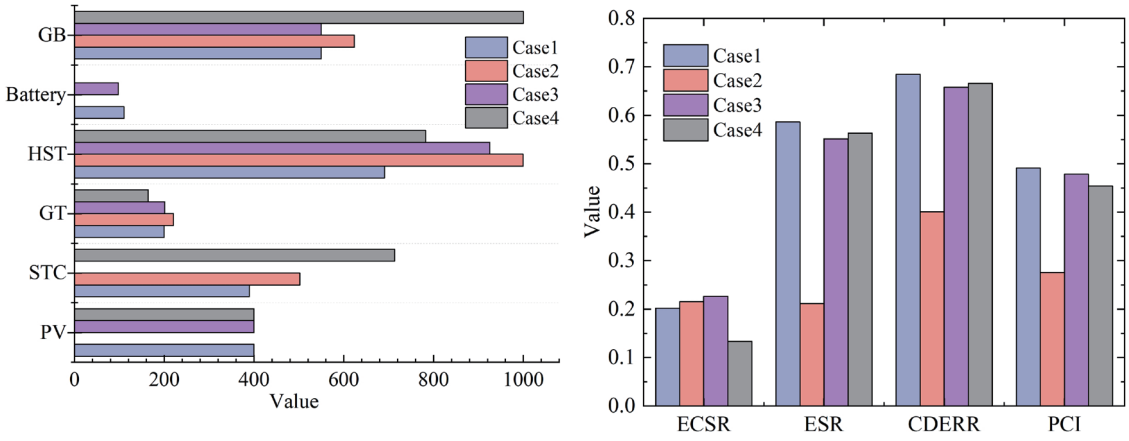

(a) (b)

Fig. 6. (Color online) (a) Configuration scheme and (b) performance evaluation index of different DESs.

greater similarity, but the HST capacity is larger in the absence of STC in the system. Figure 6(b) shows the performance evaluation index values of different DESs. Case 3 has the highest ECSR of 22.62% compared with the other cases, indicating that PV results in a lower economic efficiency of the system. This is due to the fact that although PV can reduce the fossil fuel consumption of the system for heat production, its initial investment cost is too high. For Case 4, which is not equipped with GSHP, its ECSR is only 13.34%, indicating that GSHP has the most significant impact on system economics. In terms of energy efficiency and environmental friendliness, Case 1 shows a significant advantage. The ESR of Case 1 is 58.62%, which is 37.47, 3.47, and 2.30% higher than those of Case 2, Case 3, and Case 4, respectively. The CDERR of case 1 is 68.44 %, which is 28.38, 2.65, and 1.88% higher than those of Case 2, Case 3, and Case 4, respectively. The ESR and CDERR of Case 2 are significantly lower than in the other cases, indicating that the installation of PV has the greatest impact on the energy efficiency and environmental benefits of the system. In addition, Case 1 has the highest PCI value of 49.1%, which is 21.52, 2.65, and 1.88% higher than those of Case 2, Case 3, and Case 4, respectively. Therefore, the MC-DES proposed in this paper, in which PV, STC, and GSHP are simultaneously integrated, has the best comprehensive performance.

5. Conclusions

In this study, we proposed a MC-DES in which PV, solar collector, GSHP, and sensor devices were integrated. With the objective of achieving the best economic, energy-saving, and environmental benefits, a multi-objective optimal configuration model was constructed to optimize the installed capacity of the equipment and the energy supply ratio of the GSHP. Then, a MOEDO algorithm was proposed and applied to solve the optimal configuration model. Then, four different DESs were compared to analyze the impact of different renewable energy technologies on system performance. The main conclusions of this study were as follows.

(1) Compared with the conventional SP system, the proposed MC-DES optimized by the MOEDO algorithm can save at least 20.25% of economic cost, 58.62% of fuel consumption, and 68.44% of carbon emission per year.
(2) The MOEDO algorithm enables the MC-DES to achieve better economic, environmental, and energy-saving performances. The MC-DES optimized by the MOEDO algorithm exhibits reductions of 11.58, 3.76, and 3.42% in AEC, 1.39, 10.11, and 3.44% in PEC, and 1.58, 11.20, and 4.93% in CDE compared with the MC-DESs optimized by MOEA/D, MOPSO, and NSGA-III algorithms, respectively.
(3) The introduction of PV, STC and GSHP can all effectively improve the performance of the MC-DES. GSHP has a significant impact on the economic performance of the system, while PV has a greater impact on the energy-saving and environmental performances of the system.

In this study, we proposed an MC-DES system in which sensors and renewable energy technologies were coupled, and designed a MOEDO algorithm to optimize the system configuration, providing an effective way to promote the efficient utilization of renewable energy and low-carbon operation of DESs. However, some limitations still exist. In future research, the influences of PV output uncertainty and load uncertainty on system performance

will be further investigated, and the combination of other renewable energy technologies and DES will be explored. In addition, the volatility of energy inputs and load demands have an impact on the optimal configuration of the DES, and future research will be conducted to address the multiple uncertainties that exist in the system.

Acknowledgments

This study was supported by the "Chunhui Program" Collaborative Scientific Research Project of the Ministry of Education of the People's Republic of China (Project No. HZKY20220242).

References

1 X. Y. Ren, L. L. Li, B. X. Ji, and J. Q. Liu: Energy **292** (2024) 130362. https://doi.org/10.1016/j.energy.2024.130362.
2 Z. Liu, Z. Deng, S. J. Davis, and P. Ciais: Nat. Rev. Earth Environ. **5** (2024) 253. https://doi.org/10.1038/s43017-024-00532-2
3 T. B. Nadeem, M. Siddiqui, M. Khalid, and M. Asif: Energy Strategy Rev. **48** (2023) 101096. https://doi.org/10.1016/j.esr.2023.101096
4 M. Rehan, M. Amir Raza, A. Ghani Abro, M. M Aman, I. Mohammad Ibrahim Ismail, A. Sattar Nizami, M. Imtiaz Rashid, A. Summan, K. Shahzad, and N. Ali: Energy **278** (2023) 128036. https://doi.org/10.1016/j.energy.2023.128036
5 B. X. Ji, H. H. Liu, P. Cheng, X. Y. Ren, H. D. Pi, and L. L. Li: J. Energy Storage **91** (2024) 112093. https://doi.org/10.1016/j.est.2024.112093
6 P. Rahdan, E. Zeyen, G. C. Cristobal, and M. Victoria: Appl. Energy **360** (2024) 122721. https://doi.org/10.1016/j.apenergy.2024.122721
7 M. E. Kazemian, S. A. Gandjalikhan Nassab, and E. Jahanshahi Javaran: Therm. Sci. Eng. Prog. **34** (2022) 101386. https://doi.org/10.1016/j.tsep.2022.101386
8 J. W. Lou, H. Cao, X. Meng, Y. X. Wang, J. F. Wang, L. Q. Chen, L. Sun, and M. X. Wang: Energy **289** (2024) 129963. https://doi.org/10.1016/j.energy.2023.129963
9 Z. Tian, X. Li, J. Niu, R. Zhou, F. Li: Energy. **288** (2024) 129612. https://doi.org/10.1016/j.energy.2023.129612
10 C. B. Li, H. Y. Yang, M. Shahidehpour, Z. C. Xu, B. Zhou, Y. J. Cao, and L. Zeng: IEEE Trans. Sustain. Energy **11** (2020) 2437. https://doi.org/10.1109/tste.2019.2958562
11 Z. Liu, G. Fan, D. Sun, D. Wu, J. Guo, S. Zhang, X. Yang, X. Lin, and L. Ai: Energy **239** (2022) 122577. https://doi.org/10.1016/j.energy.2021.122577
12 L. L. Li, B. X. Ji, M. K. Lim, and M. L. Tseng: Appl. Soft Comput. **150** (2024) 111087. https://doi.org/10.1016/j.asoc.2023.111087
13 R. P. Kumar and G. Karthikeyan: J. Energy Storage **75** (2024) 109702. https://doi.org/10.1016/j.est.2023.109702
14 M. Parvin, H. Yousefi, and Y. Noorollahi: Energy Convers. Manage. **277** (2023) 116639. https://doi.org/10.1016/j.enconman.2022.116639
15 S. Yang, B. L. Liu, X. L. Li, Z. Q. Liu, Y. Liu, N. Xie, and J. Z. Ren: Renewable Energy **219** (2023) 119423. https://doi.org/10.1016/j.renene.2023.119423
16 X. Y. Ren, Z. H. Wang, and L. L. Li: J. Energy Storage **86** (2024) 111214. https://doi.org/10.1016/j.est.2024.111214
17 Y. Deng, Y. Liu, R. Zeng, Q. Wang, Z. Li, Y. Zhang, and H. Liang: Energy **229** (2021) 120637. https://doi.org/10.1016/j.energy.2021.120637
18 M. Abdel-Basset, D. El-Shahat, M. Jameel, and M. Abouhawwash: Artif. Intell. Rev. **56** (2023) 9329. https://doi.org/10.1007/s10462-023-10403-9
19 Y. Li, F. Yao, S. Zhang, Y. Liu, and S. Miao: J. Energy Storage **51** (2022) 104366. https://doi.org/10.1016/j.est.2022.104366
20 X. Y. Ren, L. L. Li, B. X. Ji, and J. Q. Liu: Energy **292** (2024) 130362. https://doi.org/10.1016/j.energy.2024.130362

About the Authors

Honghao Liu received his B.Eng. degree in electrical engineering and automation from Henan University of Technology in Zhengzhou, Henan, China, in 2021. He is an M.S. student in electrical engineering at Hebei University of Technology. His research interests include integrated energy system optimization operation and intelligent optimization algorithm. (202131404081@stu.hebut.edu.cn)

Tianyu Wen received his B.Eng. degree in electrical engineering from Taiyuan University of Technology in 2021. He is an M.S. student in electrical engineering at Hebei University of Technology. His research interests include integrated energy system optimization operation and intelligent optimization algorithms. (202321401013@stu.hebut.edu.cn)

Cheng-Jian Lin received his B.S. degree in electrical engineering from Ta Tung Institute of Technology, Taipei, Taiwan, R.O.C., in 1986 and his M.S. and Ph.D. degrees in electrical and control engineering from National Chiao Tung University, Taiwan, R.O.C., in 1991 and 1996, respectively. Currently, he is a chair professor of the Computer Science and Information Engineering Department, National Chin-Yi University of Technology, Taichung, Taiwan, R.O.C. His current research interests are machine learning, pattern recognition, intelligent control, image processing, intelligent manufacturing, and evolutionary robots. (cjlin@ncut.edu.tw)

Lingling Li received her M.S. degree in control theory and control engineering in 2001 and her Ph.D. degree in electrical machinery and appliances in 2004 from Hebei University of Technology. She is currently a professor at the School of Electrical Engineering, Hebei University of Technology. Her research interests include power systems and new energy. (lilingling@hebut.edu.cn)